

## Wave transport in random systems: Multiple resonance character of necklace modes and their statistical behavior

J. Bertolotti,<sup>1</sup> M. Galli,<sup>2</sup> R. Sapienza,<sup>1</sup> M. Ghulinyan,<sup>3</sup> S. Gottardo,<sup>1</sup> L. C. Andreani,<sup>2</sup> L. Pavesi,<sup>3</sup> and D. S. Wiersma<sup>1</sup>

<sup>1</sup>*European Laboratory for Nonlinear Spectroscopy and INFM-MATIS, via Nello Carrara 1, 50019 Sesto Fiorentino, Florence, Italy*

<sup>2</sup>*Department of Physics "A. Volta," University of Pavia, Via Bassi 6, I-27100 Pavia, Italy*

<sup>3</sup>*Department of Physics, University of Trento, via Sommarive 14, I-38050 Povo, Trento, Italy*

(Received 18 January 2006; published 20 September 2006)

We present the experimental observation of multiple resonance transport of light waves, due to necklace states, in disordered one-dimensional systems. Transmission phase measurements allow us to identify these states unambiguously and investigate their statistical properties. A theoretical model is developed to describe the resonance statistics and the frequency dependence of the localization length.

DOI: [10.1103/PhysRevE.74.035602](https://doi.org/10.1103/PhysRevE.74.035602)

PACS number(s): 42.25.Dd, 05.40.Fb, 42.25.Hz, 42.55.Zz

The transport of optical waves through disordered systems can exhibit remarkable interference effects, in analogy with the transport of electrons in solids [1]. The most dramatic of all interference phenomena is maybe that of strong localization. When a random system is strongly localized, the system eigenfunctions decay exponentially (with a characteristic length  $\xi$ , called the *localization length*) thus making the diffusion coefficient vanish. This phenomenon, also known as Anderson localization, was first described for Schrödinger waves [2], but has very general validity and is now being investigated also for acoustic and electromagnetic waves [3] and very recently even degenerate atom gases [4]. Anderson localization has the extraordinary property that, when it occurs, diffusive transport comes to a halt and a disordered material starts to behave as an insulator. For optical waves the phenomenon can even be utilized to obtain laser action in a random system by using the Anderson localized states as optical cavities [5]. In three dimensions the occurrence of this phenomenon requires very strong scattering which, especially for optical systems, can only be achieved in selected materials [6]. However, in one-dimensional (1D) and two-dimensional systems it is possible to demonstrate that Anderson localization always occurs for large enough samples [7].

Surprisingly enough, and against common belief, not all modes are exponentially localized in 1D random systems, even though Anderson localization occurs. In 1987, Pendry [8] and Tartakovskii *et al.* [9] independently predicted the existence of so-called necklace modes that can appear when two or more spatially separated resonances are degenerate in energy and thus hybridize to form a band. These states are delocalized modes in an otherwise localized system and, although rare, are predicted to dominate the average transmission [10]. Evidence for the existence of necklace states was recently found in time-resolved transmission experiments [11], and subsequently also observed in experiments with microwaves [12].

In this paper we present the direct observation of multiple resonance behavior of optical necklace states via transmission measurements of the optical phase. This also allows us to determine the number of resonances that constitute each optical mode and investigate their statistical behavior. We can clearly identify necklace modes consisting of two and three resonances in a large collection of otherwise single

resonance localized modes. In addition, we develop a model that allows us to calculate the localization length analytically and predicts the number of  $n$ -order necklace modes. Theory and observations are in good agreement.

We studied, both experimentally and theoretically, binary structures composed of  $N$  dielectric layers of two types ( $A$  and  $B$ ) with different refractive indices  $n_A$  and  $n_B$  and with thicknesses  $d_A$  and  $d_B$ . In order to achieve strong scattering of light, the thicknesses were taken such that  $4n_A d_A = 4n_B d_B = \lambda_0 = 1500$  nm and the disorder was introduced by giving each layer a 50% probability to be of type  $A$  or  $B$ . The samples were realized in porous silicon (details are described elsewhere [11]). To obtain experimentally the amplitude and phase of the transmission coefficient, we performed white-light interferometry in the wavelength range 0.8–2.5  $\mu\text{m}$ . The cross-correlation interferogram of the light passing through the sample, which contains both phase and amplitude information, was measured using a fixed Mach-Zehnder interferometer coupled to a scanning Fourier-transform spectrometer [13]. Continuous phase spectra were obtained by Fourier transform of the measured interferogram followed by a standard unwrapping algorithm. The measured phase was then corrected for the delay (in vacuum) corresponding to the sample thickness, which was measured independently by a 1- $\mu\text{m}$ -resolution comparator. This yields the absolute phase delay introduced by the sample with a maximum experimental error of order of  $10^{-2}$  rad at 1.5  $\mu\text{m}$  wavelength.

In nonabsorbing systems, multiple resonant tunneling is always characterized by a phase shift of  $\pi$  per resonance. It is thus possible to discriminate necklace states from single resonances through their phase response, independently of the height of the transmission peak. In Fig. 1 the phase is plotted together with the corresponding transmission spectrum. We observed that certain transmission peaks correspond to a phase jump of multiples of  $\pi$ . These measurements provide a direct proof of the existence of second and third order necklace states in 1D random structures.

Modeling resonances as Fabry-Pérot cavities, we can approximate their line shape as Lorentzian in the limit of  $L \gg \xi$ . Considering various resonances to be independent (i.e., assuming that their spatial separation is much bigger than  $\xi$ ) we expect the line shape of necklace states to be a product of Lorentzians. Fits of the measured spectrum show good

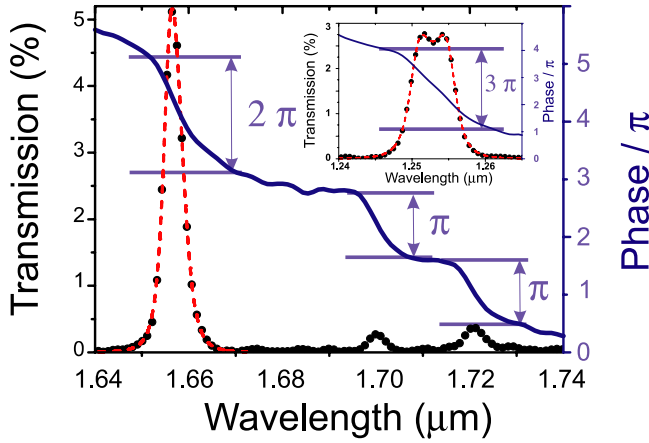


FIG. 1. (Color online) Amplitude (black dots) and phase (blue solid line) of the transmission spectrum. The second and third order necklace states were fitted, respectively, with a product of two and three Lorentzians (red dashed line).

agreement with such a model (as shown in Fig. 1). In a large series of measurements, we managed to define unambiguously the nature of 114 peaks in three samples, finding 32 second order and eight third order necklace states. Given the relatively high number of necklaces it was possible to study also their statistics.

To first order, the probability distribution  $P_m$  of necklace modes of order  $m$  can be calculated, neglecting the broadening due to mode repulsion.  $P_m$  can be estimated as the probability that  $m$  of the  $M$  resonances, in the spectral range  $S$ , superimpose within their width  $\Gamma$ , leading to

$$P_m \cong \left( \Gamma \frac{M}{S} \right)^{m-1}. \quad (1)$$

In Fig. 2 the appearance statistics calculated with this formula is compared with the experimental results.

The average extension of a localized state is of length  $\xi$ . Localized modes placed in the middle of the sample appear as the narrowest and most intense ones in the transmission spectrum. On the other side, modes that are close to the sample surface will be associated with a low and broad transmission peak. Modeling resonances as cavities in a 1D system, the relation between the intensity transmission coefficient  $T$  and the full width at half maximum  $\Gamma_1$  of a single resonance, can be calculated assuming that the angular displacement of rays is small [14]. Using the fact that outside the resonances the transmission decays as  $e^{-\ell/\xi}$ , the following parametric equations can be obtained:

$$\Gamma_1 = \frac{c}{8\pi\xi} \frac{2 - 2\sqrt{1 - e^{-(\alpha/\xi)}} \sqrt{1 - e^{-(\alpha-L)/\xi}}}{\sqrt{1 - e^{-(\alpha/\xi)}} \sqrt{1 - e^{-(\alpha-L)/\xi}}}, \quad (2)$$

$$T = \frac{e^{-L/\xi}}{(-1 + \sqrt{1 - e^{-(\alpha/\xi)}} \sqrt{1 - e^{-(\alpha-L)/\xi}})^2},$$

where  $L$  is the total length of the sample,  $c$  is the speed of light in the medium, and  $\alpha$  is a running parameter in the interval  $[\xi, L]$ . The presence of necklace modes is expected

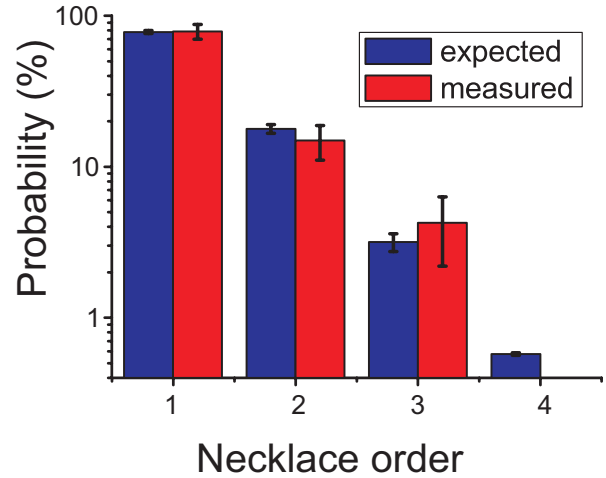


FIG. 2. (Color online) Comparison between the experimental and expected (calculated) probabilities  $P_m$  of finding a necklace mode of order  $m$  in a single 250-layer sample. Note the logarithmic scale. The error bars on the calculated values are obtained by the propagation of the uncertainty of microscopic sample parameters through the formula, while the error bar on each measured value is given by the square root of the value itself.

to produce deviations from this distribution. Due to mode coupling, necklace states are, on average, broader than single localized modes. For resonances equally spaced in the sample, the average width  $\langle \Gamma_m \rangle$  of an  $m$ th order necklace is related to the average width  $\langle \Gamma_1 \rangle$  of the single resonances as [10]

$$\langle \Gamma_m \rangle = e^{(L/2\xi)[m-1]/[m+1]} \langle \Gamma_1 \rangle. \quad (3)$$

This means that if we compare modes with the same transmission coefficient  $T$ , we expect the spectral width  $\Gamma$  of, e.g., a second order necklace mode to be about twice as large as that of a single resonance mode. The distribution of modes for various orders of necklaces should therefore be shifted to higher  $\Gamma$  at increasing order number. In Fig. 3 we have plotted the observed transmission coefficient of single resonances and double and triple necklace modes versus  $\Gamma$ , together with the theoretical behavior. Since our equations for  $\Gamma$  and  $T$  are exponentially sensitive to the exact value of  $L$  and  $\xi$ , it is not possible to accumulate enough statistics ( $\geq 1000$  sample realizations) to predict the absolute spectral width of the modes. A qualitative comparison, as in Fig. 3, shows that the relative mode broadening is well predicted, however. The data indicate that the presence of necklace states indeed produces a strong deviation (red circles and blue triangles) from the single resonance distribution (black squares) and a shift toward larger  $\Gamma$ .

An important property of necklace states is that they dominate the transmission distribution [9,10]. Since such states are relatively rare, it is necessary to use a very big ensemble to average the localization length correctly, which is not always feasible in experiments [15]. On the other hand, to compare experimental data with theory it is useful to know the actual value of  $\xi$  in order to have no free parameters. It is thus useful to develop an analytical approach to

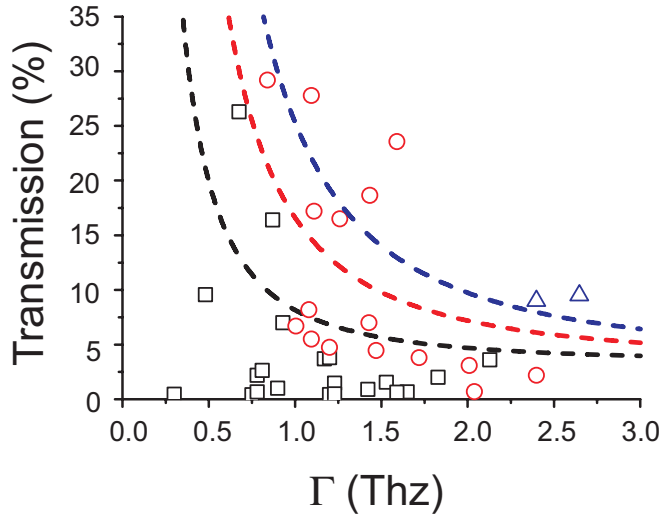


FIG. 3. (Color online) Observed distribution (in a single 250-layer sample) of transmission peaks as a function of the full width at half maximum  $\Gamma$  for single resonances (black, squares) and second and third order necklace states [respectively, red (dots) and blue (triangles)] together with the qualitative behavior obtained from the theory [black (lower) dashed line for the single cavity, red (middle) for the double cavity, and blue (upper) for the triple]. The theoretical model has no free fitting parameters.

calculate  $\xi$  over an infinitely large ensemble, i.e., evaluating all possible single and multiple resonances. At present there is still no general approach available although solutions for some particular cases were proposed [16]. Here we derive an analytical expression that relates the localization length  $\xi$  for a binary multilayer system to the microscopic sample parameters. To that end, we use the ensemble average  $\langle T^{-1} \rangle$  from the generalized second order single layer transfer matrix  $X^{(2)}$ , defined as the direct product of the two first order transfer matrices [10]:

$$X^{(2)} \equiv X \otimes X = \begin{pmatrix} \frac{1}{(t^*)^2} & \frac{2r}{|t|^2} & \left(\frac{r}{t}\right)^2 & 0 \\ \frac{r^*}{(t^*)^2} & \frac{2}{|t|^2} - 1 & \frac{r}{t^2} & 0 \\ \left(\frac{r^*}{t^*}\right)^2 & \frac{2r^*}{|t|^2} & \frac{1}{t^2} & 0 \\ 0 & 0 & 0 & 1 \end{pmatrix}, \quad (4)$$

where  $t$  and  $r$  are, respectively, the field complex transmittance and reflectance of a group of  $\mathcal{N}$  layers of the same kind ( $A$  or  $B$ ). These parameters can be easily written as a function of the refractive index and the thickness of each layer, using a standard transfer-matrix formalism [17], as

$$t_A = \frac{1}{\cos\left(2\pi\mathcal{N}\frac{n_A d_A}{\lambda}\right) - i\left(\frac{n_B^2 + n_A^2}{2n_A n_B}\right)\sin\left(2\pi\mathcal{N}\frac{n_A d_A}{\lambda}\right)},$$

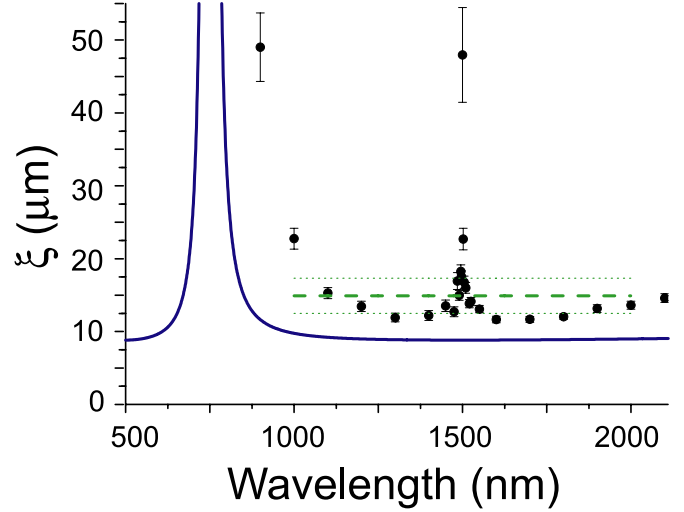


FIG. 4. (Color online) Numerical (black dots) and analytical (blue, solid line) prediction for  $\xi$  are compared with the experimental result (green, dashed line). The experimental value is averaged over frequency (in the interval 1–2  $\mu\text{m}$ ) and thus is wavelength independent. The green dotted lines represent the experimental uncertainty for  $\xi$ .

$$r_A = \frac{-i\left(\frac{n_B^2 - n_A^2}{2n_A n_B}\right)\sin\left(2\pi\mathcal{N}\frac{n_A d_A}{\lambda}\right)}{\cos\left(2\pi\mathcal{N}\frac{n_A d_A}{\lambda}\right) - i\left(\frac{n_B^2 + n_A^2}{2n_A n_B}\right)\sin\left(2\pi\mathcal{N}\frac{n_A d_A}{\lambda}\right)}, \quad (5)$$

where  $\lambda$  is the vacuum wavelength. Transmittance  $t_B$  and reflectance  $r_B$  have the same functional form but with the indices  $A$  and  $B$  exchanged.

Assuming that the layers are uncorrelated, the average of the total transfer matrix  $X_{tot}^{(2)}$  over all possible realizations of the disorder can be written as the product of the transfer matrices  $X_j^{(2)}$  of the individual layers:  $\langle X_{tot}^{(2)} \rangle = \prod_{j=1}^{\mathcal{N}} \langle X_j^{(2)} \rangle = \langle X_j^{(2)} \rangle^{\mathcal{N}}$ . In our case the ensemble average is obtained by averaging  $X^{(2)}$  over the type of layer and over  $\mathcal{N}$ . In Eq. (5) it is shown that  $r$  is antisymmetric for the exchange of  $A$  and  $B$ ; i.e., in the average type of layer, all terms linear in  $r$  or  $r^*$  in Eq. (4) become identically zero for all wavelengths. We can thus write  $2\langle T^{-1} \rangle = ([X^{(2)}]_{2,2})^{\mathcal{N}} + 1$ . Since  $\ln\langle T^{-1} \rangle = 2L/\xi$  [18], solving this equation and averaging over  $\mathcal{N}$  leads to the following analytical expression:

$$\xi(\lambda) = \frac{2L}{\ln\langle T^{-1} \rangle} = 2(d_A + d_B) \left[ \ln\left( (3n_A^2 + n_B^2)(n_A^2 + 3n_B^2) + 3\frac{(n_A^2 - n_B^2)^2}{4\cos(\pi(\lambda_0/\lambda)) - 5} \right) - 2\ln(4n_A n_B) \right]^{-1}. \quad (6)$$

This function is plotted in Fig. 4 together with the wavelength averaged experimental value (averaged between  $\lambda = 1$  and 2  $\mu\text{m}$ ) of  $\xi = 14.9 \pm 2.4 \mu\text{m}$  (obtained elsewhere for the same sample [11]). Close to  $\lambda = 750 \text{ nm} = \lambda_0/2$ , the localization length  $\xi$  diverges since this corresponds to an optical thickness of half the wavelength of all layers and the sample is therefore transparent for all realizations of disorder. In

other words, at this wavelength scattering is absent and all states are therefore extended. Vice versa, if the system is completely disordered, one expects the scattering to be strongest at  $\lambda=\lambda_0$  when the optical thickness of the layers is  $\lambda/4$ , obtaining thus a minimum in  $\xi$ .

In addition, we calculated numerically the transmission values at various thicknesses, solving the transfer matrix numerically, for many realizations of the disorder. We estimated the localization length by fitting the equation  $\langle \ln T \rangle = -\xi/L$  to the transmission values. These numerical results are plotted as dots in Fig. 4 together with the confidence interval of the fit. Note that the numerical results on a finite-size sample show a peak of  $\xi$  at  $\lambda=\lambda_0$ . It is known that residual order can give rise to anomalies in the localization length [19]. Due to the quarter-wavelength condition imposed on the layer thicknesses, a hidden order is contained in the system because, at  $\lambda_0$ , each pair of equal layers (like *AA* or *BB*) has an optical thickness of  $\lambda/2$  and is therefore equivalent to the identity matrix (i.e., its transmission coefficient is 1 and the phase shift a multiple of  $2\pi$ ) [20]. Our analytical formula does not consider the possibility of residual order in the system and therefore does not show these finite-size effects.

In conclusion we managed, through transmission mea-

surements of the optical phase, to identify multiple resonance transport and to characterize unambiguously the order of each necklace resonance. The sensitivity of this technique allows us to study the necklace statistics and compare the experimental data with a simple theoretical model. Good agreement is obtained. We calculated, both analytically and numerically, the frequency dependence of the localization length  $\xi$  in binary disordered multilayers with positional disorder, developing a model to evaluate  $\xi$  and unveiling surprising properties like finite-size anomalies and hidden partial order. Our results are of general validity for all wave transport phenomena in random 1D systems, including sound and seismic waves, fonons (heat transport), electrons, and degenerate matter waves, as the propagation of a Bose-Einstein condensate or Fermi sea.

We wish to thank John Pendry, Maurizio Artoni, Costanza Toninelli, Roberto Righini, and Marcello Colocci for discussions. The work was supported by MIUR through the Cofin project ‘‘Silicon-Based Photonic Crystals,’’ by the EC (LENS) under Contract No. RII3-CT-2003-506350, and by the EU through Network of Excellence IST-2-511616-NOE (PHOREMOST).

- 
- [1] See, e.g., Ping Sheng, *Introduction to Wave Scattering, Localization, and Mesoscopic Phenomena* (Academic Press, New York, 1995); *Photonic Crystals and Light Localization in the 21st Century* edited by C. M. Soukoulis (Kluwer, Dordrecht, 2001); *Wave Scattering in Complex Media: From Theory to Applications*, edited by B. A. van Tiggelen and S. E. Skipetrov (Kluwer, Dordrecht, 2003).
- [2] P. W. Anderson, *Phys. Rev.* **109**, 1492 (1958).
- [3] S. John, *Phys. Rev. Lett.* **53**, 2169 (1984); P. W. Anderson, *Philos. Mag. B* **52**, 505 (1985); K. Arya, Z. B. Su, and J. L. Birman, *Phys. Rev. Lett.* **57**, 2725 (1986); A. Lagendijk, M. P. v. Albada, and M. P. v. d. Mark, *Physica A* **140**, 183 (1986).
- [4] H. Gimpferlein, S. Wessel, J. Schmiedmayer, and L. Santos, *Phys. Rev. Lett.* **95**, 170401 (2005); D. Clément *et al.*, *ibid.* **95**, 170409 (2005); C. Fort *et al.*, *ibid.* **95**, 170410 (2005).
- [5] P. Pradhan and N. Kumar, *Phys. Rev. B* **50**, 9644 (1994); V. Milner and A. Z. Genack, *Phys. Rev. Lett.* **94**, 073901 (2005).
- [6] R. Dalichaouch *et al.*, *Nature (London)* **354**, 53 (1991); D. S. Wiersma *et al.*, *ibid.* **390**, 671 (1997); A. A. Chabanov and A. Z. Genack, *Phys. Rev. Lett.* **87**, 233903 (2001).
- [7] N. F. Mott and W. D. Twose, *Adv. Phys.* **10**, 107 (1961); D. J. Thouless, *Phys. Rev. Lett.* **39**, 1167 (1977).
- [8] J. B. Pendry, *J. Phys. C* **20**, 733 (1987).
- [9] A. V. Tartakovskii *et al.*, *Sov. Phys. Semicond.* **21**, 370 (1987).
- [10] J. B. Pendry, *Adv. Phys.* **43**, 461 (1994).
- [11] J. Bertolotti, S. Gottardo, D. S. Wiersma, M. Ghulinyan, and L. Pavesi, *Phys. Rev. Lett.* **94**, 113903 (2005).
- [12] P. Sebbah, B. Hu, J. M. Klosner, and A. Z. Genack, *Phys. Rev. Lett.* **96**, 183902 (2006).
- [13] M. Galli, F. Marabelli, and G. Guizzetti, *Appl. Opt.* **42**, 3910 (2003); M. Galli, D. Bajoni, F. Marabelli, L. C. Andreani, L. Pavesi, and G. Pucker, *Phys. Rev. B* **69**, 115107 (2004).
- [14] See, e.g., O. Svelto, *Principles of Lasers* (Springer Science, New York, 1998).
- [15] P. W. Anderson, *Nobel Lectures in Physics, 1971–1980* (World Scientific, Singapore, 1992).
- [16] K. Y. Bliokh and V. D. Freilikher, *Phys. Rev. B* **70**, 245121 (2004).
- [17] See, e.g., F. J. Pedrotti and L. S. Pedrotti, *Introduction to Optics* (Prentice-Hall, Englewood, Cliffs, NJ, 1992).
- [18] J. A. Sañchez-Gil and V. Freilikher, *Phys. Rev. B* **68**, 075103 (2003); K. Yu. Bliokh, Yu. P. Bliokh, and V. Freilikher, *J. Opt. Soc. Am. B* **21**, 113 (2004).
- [19] M. Titov and H. Schomerus, *Phys. Rev. Lett.* **95**, 126602 (2005).
- [20] At this wavelength, a random sequence like *BAABBAABBABAAAABAAAABBBBBBABAB* can be simplified to *BABBAABAB* and subsequently to *BABAB* by removing pairs of layers *AA* and *BB* that are optically transparent. An irreducible sequence is obtained when all such pairs of optical thickness  $\lambda/2$  have been removed, leaving an alternating *AB* structure. Hence the finite-size random stack of layers *A* and *B* is equivalent to a periodic system at, and, for a finite-size system, in a narrow wavelength band around,  $\lambda_0$ .